Applied Thermal Engineering 108 (2016) 1320–1335

Contents lists available at ScienceDirect

Applied Thermal Engineering

journal homepage: www.elsevier.com/locate/apthermeng

Research Paper

An integrated A/C and HDH water desalination system assisted by solar energy: Transient analysis and economical study

A. Fouda [a,*], S.A. Nada [b], H.F. Elattar [b]

[a] Department of Mechanical Power Engineering, Faculty of Engineering, Mansoura University, 35516 El-Mansoura, Egypt
[b] Department of Mechanical Engineering, Benha Faculty of Engineering, Benha University, Benha, 13511 Qalyubia, Egypt

HIGHLIGHTS

- Hybrid A/C and HDH desalination system solar assisted are proposed.
- Transient analysis and parametrical study for system performance are presented.
- Effects of operating and design parameters on the proposed system is investigated.
- System capacity, consumption, performance and cost saving analysis are hourly and daily investigated and presented.
- Proposed system operates more efficient in more hot and humid climatic conditions.

ARTICLE INFO

Article history:
Received 1 June 2016
Revised 31 July 2016
Accepted 3 August 2016
Available online 4 August 2016

Keywords:
Integrated system
Solar energy
A/C
HDH
Hot and humid climates

ABSTRACT

Theoretical investigation on the performance of a proposed innovated solar integrated system for air conditioning (A/C) and humidification dehumidification (HDH) water desalination in hot and humid regions is presented. Transient analysis and parametrical study for the system are conducted under different operating and design conditions. System performance parameters (fresh water production rate, cooling capacity, electrical power consumption, water recovery and system coefficient of performance) are hourly estimated and daily integrated for different operational and design conditions. The results reveal the increase of fresh water productivity, system water recovery, cooling capacity, electrical power consumption and COP of the system with the increase of air temperature, air humidity, and solar collectors area. For system assessment, the system performance parameters are compared with the performance of a basic system under the same conditions. Cost saving analysis showed the proposed system operates more economically and efficiently that in hot and humid climatic areas. General numerical correlations for system performance parameters are proposed in terms of the design and operational conditions.

1. Introduction

Air conditioning and fresh water are necessary for life permanency and nations development including agricultures and industries activities. Fresh water and fossil fuel sources are dramatically depleting due to the rapid increase in world population and the demands of recent life activities. Water desalination can be considered as a solution of fresh water sources depletion but it consumes a considerable amount of energy. Moreover, air conditioning systems consume considerable electrical energy specially in hot and humid areas. The use of fossil fuel for electricity generation and drive water desalination and air conditioning systems is not sustainable as they harm environment and accelerate fuel depletion. Using renewable energy sources especially solar energy can be considered as a solution of these problems. Recently, integrated A/C and water desalination system using HDH approach derived by mechanical vapor compression (MVC) and solar energy are proposed as an efficient solution for fossil fuel saving, fresh water production and environment protection. HDH desalination and A/C hybrid system is simple in design, construction and operation and appropriate for developing countries which suffer form energy and fresh water lacks problems. A broad survey on uses renewable energy-driven technologies of integrated desalination systems was presented by Ghaffour et al. [1]. A small scale solar HDH system using glass evacuated tubes solar air heater was studied and presented by Li et al. [2]. Yıldırım and Solmus [3] theoretically investigated the performance of HDH water desalination system driven by solar energy for Antalya, Turkey under different design and operational parameters. El-Agouz et al. [4] designed and

* Corresponding author.
E-mail address: eng_alifouda@mans.edu.eg (A. Fouda).

http://dx.doi.org/10.1016/j.applthermaleng.2016.08.026
1359-4311/

Nomenclature

A	area, m^2
A/C	air conditioning
ADP	apparatus dew point
COP	coefficient of performance
C_p	specific heat, kJ/kg K
EES	engineering equations solver
$E^{\bullet}$	total electric power, kW
$E_{ps,day}$	daily total electric energy, kW h
FAR	fresh air ratio
FWST	fresh water storage tank
L	latitude angle, °
H	hour angle, °
HDH	humidification-dehumidification
h_{fg}	water latent heat of evaporation, kJ/kg
i	specific enthalpy, kJ/kg
I_T	total solar intensity, W/m^2
$m^{\bullet}$	mass flow rate, kg/s
$m_{w,day}$	daily fresh water production, kg
$Q^{\bullet}_{cc}$	cooling coil capacity, kW
$Q^{\bullet}_{R}$	building cooling load, kW
$Q_{R,day}$	daily building cooling energy, kW h
R	system water recovery
RSHF	room sensible heat factor
TOCS	total operating cost saving
P_s	saturation pressure, Pa
t	temperature, °C
W	absolute humidity, kg_v/kg_a
$W^{\bullet}_{c}$	compressor power, kW

Greek symbols

β	tilt angle, °
δ	declination angle, °
η	efficiency
ψ	arbitrary variable

Subscript

a	air
atm	atmosphere
BS	basic system
cc	cooling coil
cond	condensate
cw	cold water
deh	dehumidifier
h	humidifier
i	inlet
inp	input
m	mean
o	outlet
R	room condition
Ref	refrigeration
Re	recirculate
RH	relative humidity
PS	proposed system
S	supplied state of conditioned space
s	saturation state
SC	solar collector
v	water vapor
w	water

constructed a pilot plant in a dry area using solar water collector to increase fresh water production from salty water. Sharon and Reddy [5] performed a review for various desalination units driven by renewable energy particularly solar energy. Kabeel and El-Said [6] investigated and compared various configurations of hybrid desalination systems based on air HDH–single stage flashing and powered by solar energy. Shatat et al. [7] presented theoretical study on small scale HDH water desalination unit integrated with an evacuated tube solar collector.

Kumar et al. [8] developed thermal model to predict the performance of a single slope solar still integrated with evacuated tube collector under New Delhi (India) climatic conditions. Liu et al. [9] presented thermal and economic analyses for water desalination system using evacuated tube solar collectors. Al-Sulaiman et al. [10] presented thermodynamic analysis to evaluate the performance of HDH system integrated with parabolic trough solar collector (PTSC). Hawlader [11] studied the influences of supply water temperature and flashing on the performance of a new desalination system operated with solar heat pump. Yuan et al. [12] proposed an integrated system for A/C and water desalination using humidification-dehumidification process and assisted by MVC heat pump. An open air MVC refrigeration unit for hybrid A/C and water desalination system for ship was presented by Houa et al. [13]. Habeebullah [14] conducted experimentally the performance analysis for an integrated heat pump with a dehumidification technique for fresh water producing from atmospheric air. The unit serve an office building with 250 m^2 area and air supply capacity of 1.586 m^3/s, the building located on the sea in Jeddah city, KSA, where the mean atmospheric temperature and relative humidity are 34 °C and of 71%, respectively. Jain and Hindoliy [15] conducted performance study for two different pad materials used in evaporative cooling (coconut and plash fibers) and compared their performance with the traditional aspen and khus pads. Halima et al. [16] studied theoretically the performance of a simple solar still integrated with a heat pump. Al-Enezi et al. [17] examined and investigated the performance of water desalination system using HDH technique at low operational temperatures. The maximum fresh water rate was observed at elevated hot water and low cooling water temperatures and at high air and low hot water mass flow rates. Nafey et al. [18] performed theoretical and experimental studies for solar water desalination unit by utilizing flashing process on a small scale unit. The fresh water productivity was calculated by developing a mathematical model under various operating conditions. The mean summer water productivity obtained varied from 5.44 to 7 kg/day/m^2 in July and August and from 4.2 to 5 kg/day/m^2 in June. Mohamed and El-Minshawy [19] presented simulation modeling to assess the performance of seawater HDH water desalination system driven by solar energy. The model was built with comparison study to display the influence of the various operating conditions on the system performance and fresh water production. Ghazal et al. [20] constructed an experimental setup to enhance the solar Humi dification-Dehumidification Desalination (HDD) systems performance. The air and water solar heaters and the traditional HDD evaporator were substituted with compact system. It was observed that a direct contact bubbling humidification is an efficient method in HDD systems. Dayem and Fatouh [21] accomplished theoretical and experimental investigation for various HDH solar assisted water desalination systems to present the best efficient system. Three systems were suggested and compared for climatological environments of Cairo (30°N). Hermosillo et al. [22] presented theoretical and experimental work on a novel suggested HDH desalination system. The evaporator was manufactured from treated cellulose paper in which water was evaporated. He et al. [23]

carried out a parametrical study on HDH water desalination system utilizing low grade heat sources for seawater heating prior the humidifier. The desalination system performance and the low grade heat collector type were studied at various operating pressures. Chiranjeevi and Srinivas [24] carried out experimental and simulation study to develop and analyze two stages HDH desalination and cooling hybrid system to prove the probability of improving the desalination yield with supplemented cooling support. Giwa et al. [25] investigated HDH desalination system powered by photovoltaic system for fresh water and electricity production in climatic conditions of Abu Dhabi, UAE. Buker et al. [26] developed and tested pilot scale experimental set-up for to present effect of the different parameters such as weather condition, air flow and regeneration temperature on the proposed system performance. Using photovoltaic/thermal roof collector combined with a liquid desiccant. The results confirmed the potential of the examined technology, and explained the specific conclusions for the practice of such systems. Nada et al. [27] achieved an experimental study to investigate the performance of an integrated HDH water desalination and A/C system using vapor compression refrigeration unit. Recently, Nada et al. [28] studied theoretically the performance of integrated A/C and water desalination systems using HDH technique suggested for hot and dry weather areas. Four systems with evaporative cooler and heat recovery units were employed, analyzed and assessed at various operating conditions. Elattar et al. [29] presented parametrical and economical study of the performance of integrative A/C and HDH water desalination system assisted by solar energy. The system performance was investigated under steady-state operation utilizing solar thermal storage and auxiliary heating units.

According to the above literature and the authors' review, researches on combined solar-assisted systems driven by MVC chiller for A/C and HDH water desalination are still needed to investigate the effects of operational and design system parameters on the system performance. Energy saving, fresh water recovery, human thermal comfort issues and numerical correlations for system performance parameters are not addressed in the previous researches. Therefore, the goal of the present work is a performance investigation of a combined A/C and HDH water desalination system assisted by solar energy. A new configuration of the system is presented. The system performance parameters: system capacity, consumptions and performance parameters are instantaneously and daily integrated investigated for different operational and design system parameters (solar intensity, ambient air temperature, ambient absolute humidity, ambient air flow rate, fresh air ratio, solar collectors' areas, dehumidifier cooling water mass flow rate, humidifier water mass flow rate and dehumidifier cooling water temperature). The system is tested under the conditions of hot and humid climatic cities; namely under the meteorological data of Jeddah city in KSA. Hourly and daily performance of the system are analyzed at various operational and design system parameters. The modeling of the system performance is developed based on heat and mass balances and solved by using Engineering Equation Solver (EES) software and C++ programming language. For system assessment, the performance and productivity of the presented system are compared with the basic air conditioning system. Cost saving analysis is also presented in the form of total operating cost saving (TOCS) due fresh water productivity and saving in electric power consumption. General numerical correlations for hourly fresh water productivity, space cooling load and total electrical power consumption for the proposed system are correlated as a function in the system design and operational parameters.

2. Systems description

Fig. 1 illustrates a schematic diagram for a basic air conditioning central system which is used as a reference system to assess the performance of the proposed hybrid system. The basic system consists of mainly cooling/dehumidifying coil and air cooled chiller unit to support the air conditioning of a building. A water chemical treatment unit is used to treat the condensate water to be fresh water. Ambient air (O) is mixed with recirculated air (R). The mixed air (M) is then passed on a cooling coil where it is cooled and dehumidified (S). The condensate water passes through a chemical water treatment unit where it is treated to be fresh water.

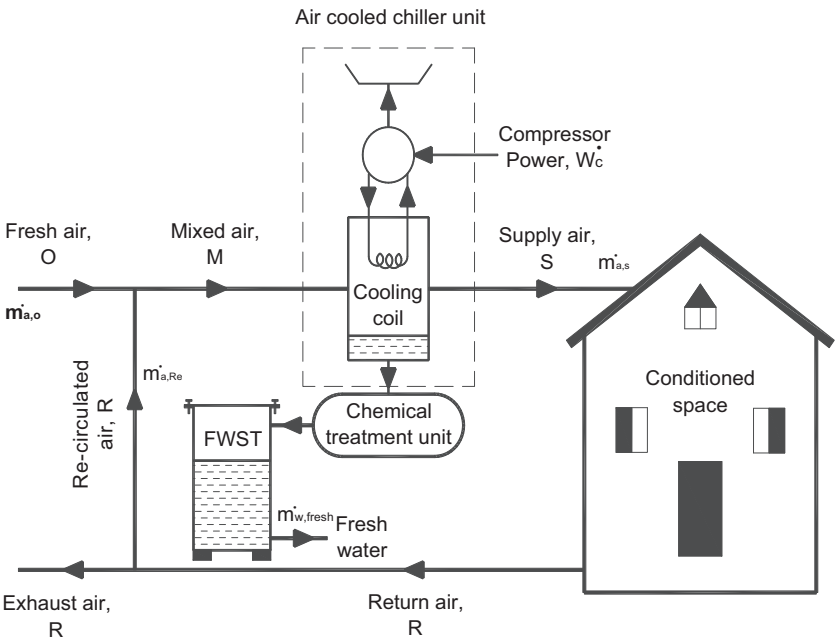

Fig. 1. Basic system schematic.

The schematic diagram of the proposed hybrid integrated system is given in Fig. 2. The main system components are: air and water solar collectors, humidifier, dehumidifier, air cooled chiller unit and chemical water treatment units. Air is drawn from ambient (O) to flow into air solar collector, where it is sensibly heated (L). The air is then humidified in the humidifier (H) by spraying the hot water that received from the water solar collector. The Air and water solar collectors are used to rise the air humidification

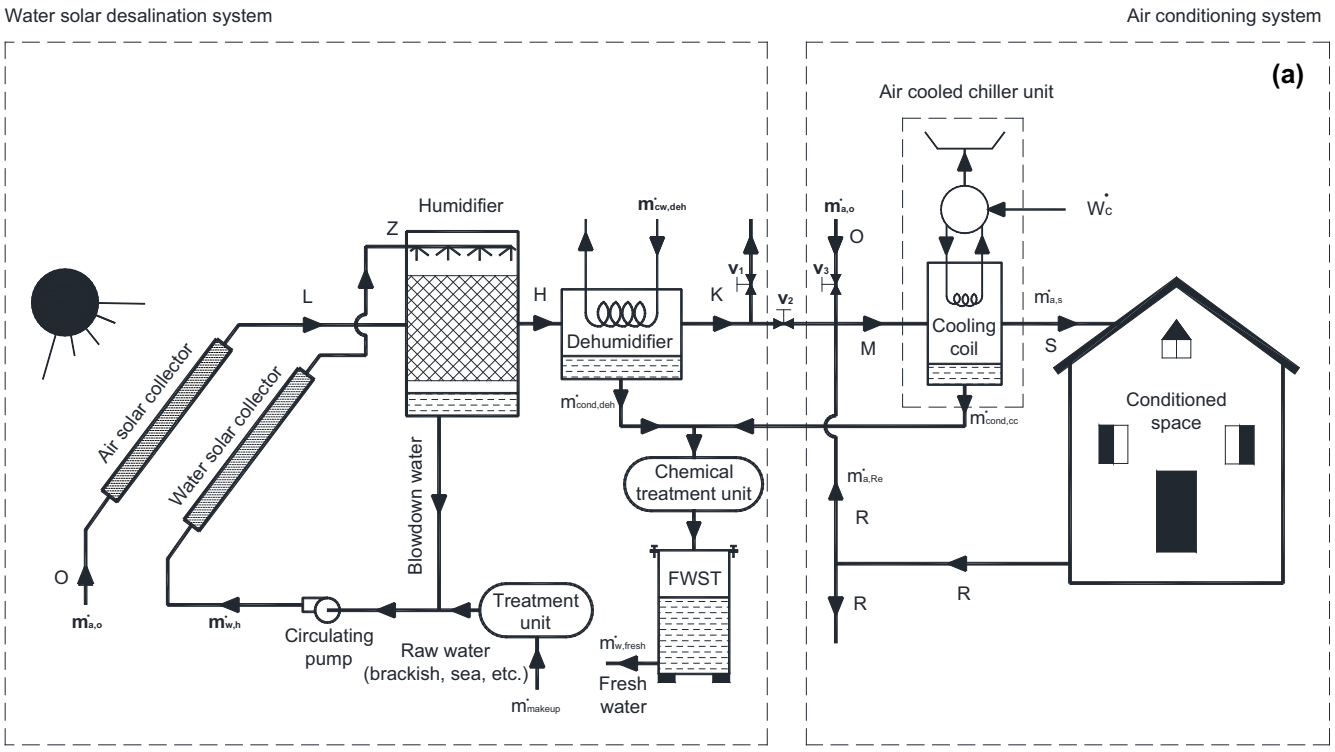

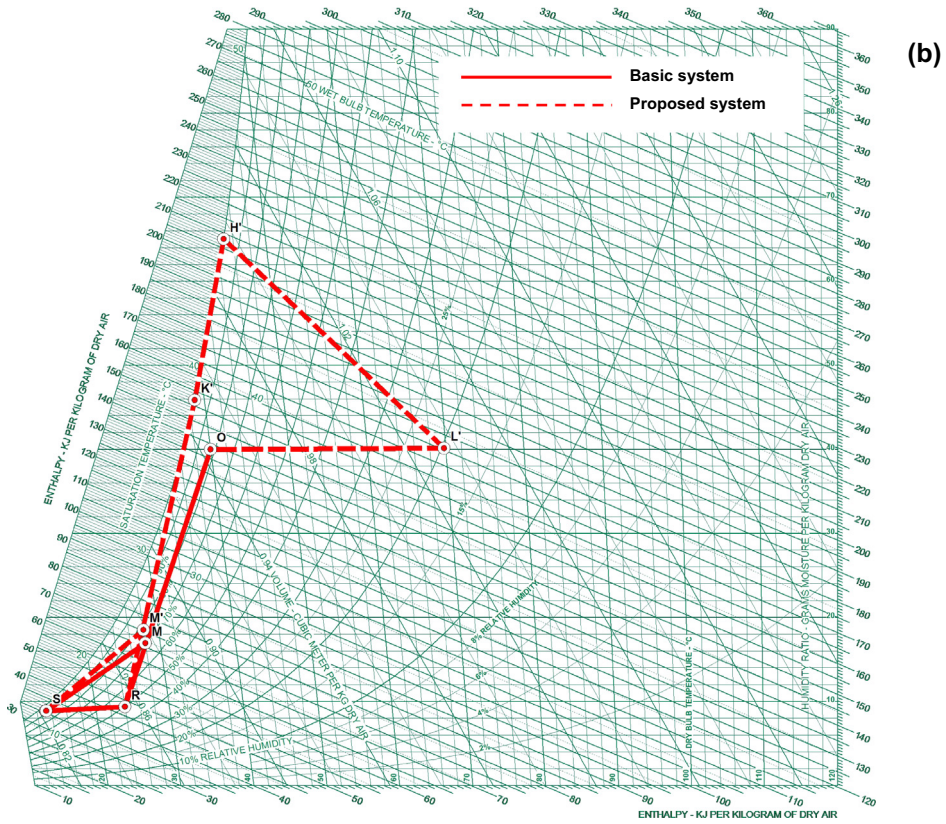

Fig. 2. Proposed system: (a) schematic, (b) psychrometric cycles.

capacity by elevating the air and sprayed water temperatures. The humidified air is then cooled and dehumidified (K) through the dehumidifier. The water condensate on the dehumidifier surface are drained to the water treatment section to produce fresh water. The dehumidified air is then mixed with the recirculated air (R). The mixed air (M) is then passes through the cooling coil of the air condition system to be cooled and dehumidified (S) producing additional fresh water. Chilled water comes from air cooled chiller unit passes in the cooling coil unit to maintain coil apparatus dew point (ADP) of 7 °C. Finally, the cooled and dehumidified air (S) is supplied to the conditioned space to remove the cooling load and cool the space. Fig. 2b displays the psychrometric processes of air cycles for basic and proposed systems.

In the humidifier, brackish/sea water is treated in the treatment unit and is then pumped and sprayed in the humidifier after heating it in the solar water collector. Part of the sprayed water is evaporated and carried up by the humidified air and the remaining amount is recirculated and mixed with make-up water (sea/brackish water). In the dehumidifier, a cooling water (sea/brackish) with temperature lower than dew point temperature of the air at point (H) is used to dehumidify the air. The condensate water is then drawn and flowed into chemical treatment unit and finally kept in fresh water storage tank (FWST).

The suggested integrated system may be operated with three various manners; water desalination system only, A/C system only, and combined A/C and water desalination system. In case of using it as water desalination system only, the system works under shutting valve $\mathbf{V_2}$ and opening valve $\mathbf{V_1}$ to exclude the A/C cycle for whole system. While, in case of using it as A/C system only, the system is operated by closing the valve $\mathbf{V_2}$ and open the valve $\mathbf{V_3}$ to exclude the water desalination cycle from whole system. In case of a combined A/C and water desalination system both A/C and desalination cycles are operating in the same time by closing valves $\mathbf{V_1}$ & $\mathbf{V_3}$ and opening valve $\mathbf{V_2}$. The current study is investigated under combined modes using fully solar utilization in desalination system during daylight hours.

3. Thermodynamic analysis and numerical modeling

A numerical model for the presented system is developed using energy and mass balance equations for the system components. The model is developed based on the following assumptions:

- Leakage (air/water) in the system components are neglected.
- The water temperature leaving the humidifier is similar to air wet-bulb temperature leaving it.
- Humidifier efficiency is 100% (i.e. air is leaving the humidifier as saturated air).
- The process through the dehumidifiers is along the saturation curve.
- The produced fresh water, cooling water and air dry-bulb temperatures are equal at the dehumidifier exits.
- Specific power of auxiliary components (power consumed by fans and pumps per unit amount of fresh water rate) is assumed as 0.029 kW/($m^3_{w,fesh}$/h) [30,31].
- Water vapor at the humidifier outlet is free salt [32], therefore the condensate water need a chemical treatment to be fresh/potable water with salinity 500 ppm according to the WHO (World Health Organization) as a recommended value.
- Thermal comfort conditions of the conditioned space are $T_{db,R}$ = 24 °C and RH = 50%.
- Cooling coil surface temperature and RSHF are chosen as 7 °C and 0.9, respectively as typical values for hot and humid climates.

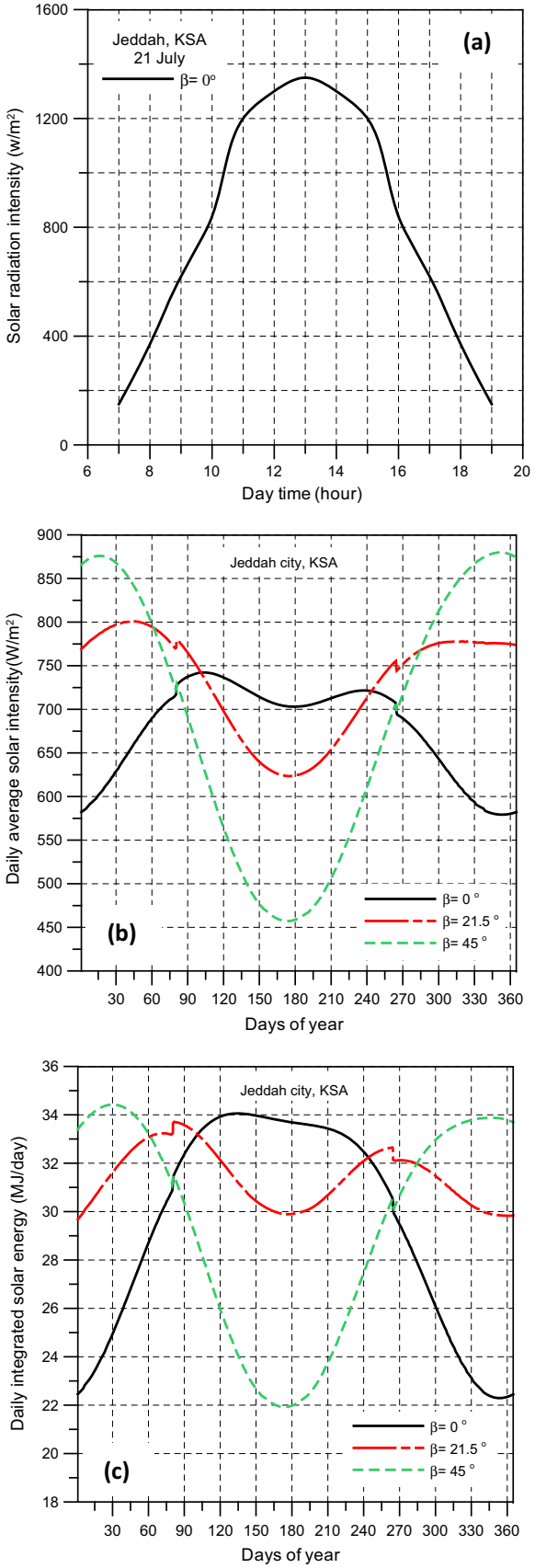

Fig. 3. Solar radiation intensity: (a) solar intensity during the daylight, (b) daily average solar intensity during a year, (c) daily integrated solar energy during a year.

Fresh water productivity, system cooling capacity, system electrical power consumption, system water recovery and entire system coefficient of performance are expressed as a function in the operating and design system parameters.

3.1. Solar collectors

Solar radiation is a main parameter in the proposed hybrid solar system. The hourly total solar radiation incident on the air and water solar collectors are calculated according to the local geographical coordinates of Jeddah city, KSA. The total solar radiation I_T on a tilted surface is calculated as the sum of direct, diffuse and reflected radiations as follows:

$$I_T = I_b + I_d + I_r \tag{1}$$

where I_b, I_d and I_r are the direct, diffuse and reflected components of the solar radiation, respectively. I_T *is* also presented by Duffie and Beckman [33] as follows.

$$I_T = I_b R_b + I_d \frac{1+\cos\beta}{2} + (I_b + I_d)\rho_g \frac{1-\cos\beta}{2} \tag{2}$$

where ground reflectance ρ_g equals 0.2 and R_b (tilt factor of beam radiation) for the specific case of a south-facing fixed surface with a tilt angle of β, is

$$R_b = \frac{\sin(L-\beta)\sin(\delta) + \cos(L-\beta)\cos(\delta)\cos(h)}{\sin(\delta)\sin(L) + \cos(\delta)\cos(h)\cos(L)} \tag{3}$$

where L, δ, and h are the latitude, declination and hour angles, respectively. Detailed calculation procedures for the I_T and R_b are given by Duffie and Beckman [33]. According to the preceding equations the solar radiation intensity, daily average and integrated solar radiation intensity and energy are calculated and illustrated in Fig. 3a–c, respectively for Jeddah city. As shown in Fig. 3b and c, the optimum path of solar intensity during the year can be obtained from intersected lines of different tilt angles.

The calculated solar intensity is related to the temperature rise by the solar collector efficiency equation as suggested by Yuan and Zhang [34].

$$\eta_{SC} = \frac{m^{\bullet} c_p (t_{SC,o} - t_{SC,i})}{I_T A_{SC}} \tag{4}$$

The following empirical correlations for solar collector efficiency which was presented by [1,35] are used with Eq. (4) to calculate air and water temperatures downstream the solar collectors.

$$\eta_{w,SC} = a_1 + a_2 \frac{t_{SC,i} - t_{w,o}}{I_T} \tag{5}$$

$$\eta_{a,SC} = a_1 + a_2 \frac{t_m - t_{a,o}}{I_T} \tag{6}$$

where $a_1 = 0.37$, $a_2 = -3.35$ and $t_m = \frac{t_{SC,o}+t_{SC,i}}{2}$.

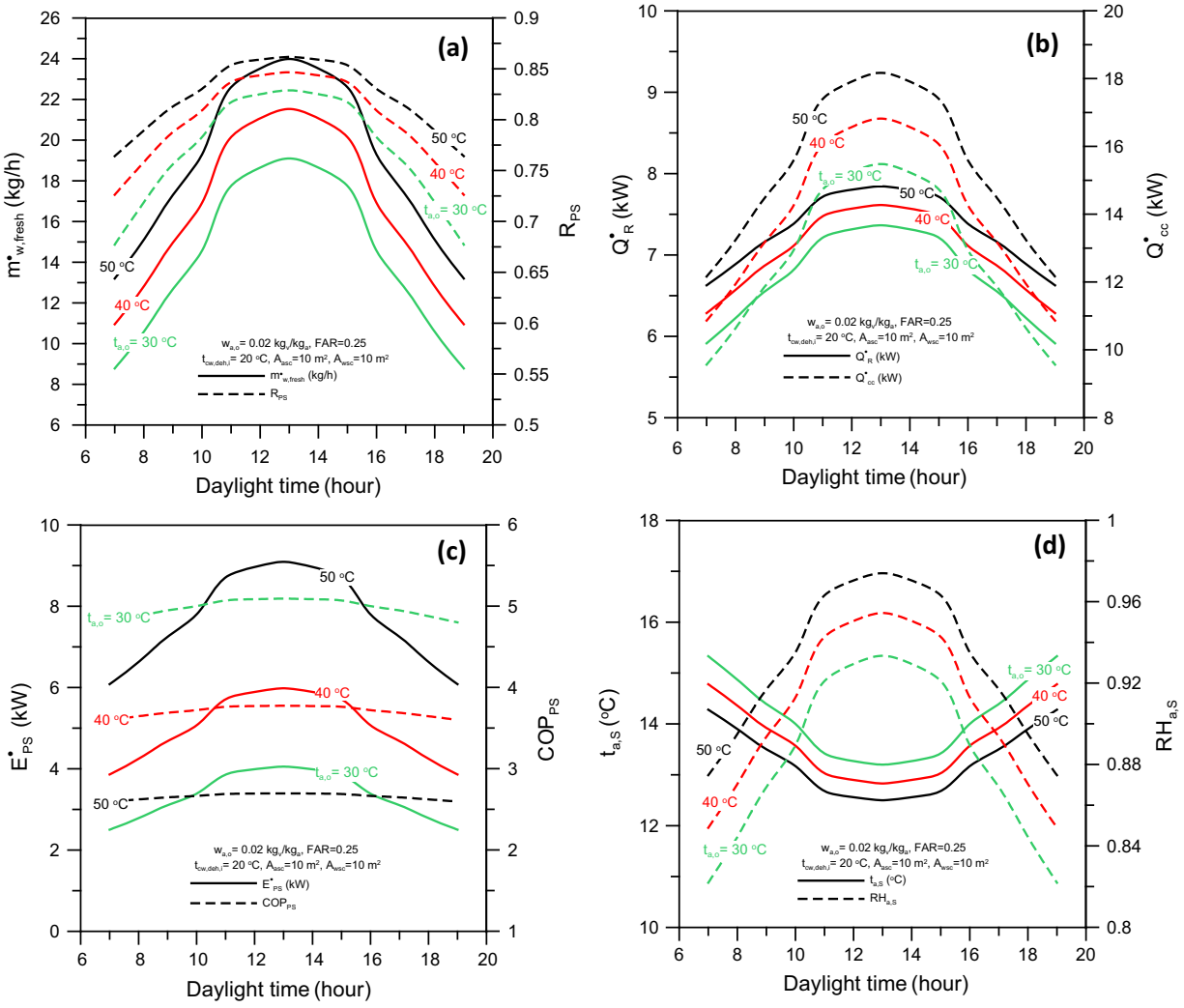

Fig. 4. Influences of ambient air dry bulb temperature on the proposed system performance parameters: (a) $m^{\bullet}_{w,fresh}$ & R, (b) $Q^{\bullet}_R$ & $Q^{\bullet}_{cc}$, (c) $E^{\bullet}_{ps}$ & COP_{PS}, (d) $t_{a,s}$ & $RH_{a,s}$.

3.2. Humidifier

Energy balance of the humidifier is

$$m^{\bullet}_{a,o}(i_{a,h,o} - i_{a,h,i}) = m^{\bullet}_{w,h,i}c_{p,w}t_{w,h,i} - m^{\bullet}_{w,h,o}c_{p,w}t_{w,h,o} \quad (7)$$

The absolute humidity of the inlet air to solar air collector is given by

$$w_s = \frac{0.622RHP_s}{P_{atm} - RHP_s} \quad (8)$$

where P_s is the water vapor saturation pressure and is given by [36]:

$$P_s = \exp\left(23.196 - \frac{3816.44}{T_a - 46.13}\right) \quad (9)$$

The air specific enthalpy is calculated by summing of the sensible and latent parts as follows:

$$i_a = c_{p,a}t_a + w(2500 + 1.84t_a) \quad (10)$$

The mass flow rate of the makeup water (sea or brackish) supplied to the system is given by:

$$m^{\bullet}_{makeup} = m^{\bullet}_{a,o}(w_{a,h,o} - w_{a,h,i}) \quad (11)$$

3.3. Dehumidifier

Energy balance of the dehumidifier can be expressed as.

$$m^{\bullet}_{a,o}(i_{a,deh,i} - i_{a,deh,o}) = m^{\bullet}_{cw,deh}c_{p,w}(t_{cw,deh,o} - t_{cw,deh,i}) + m^{\bullet}_{cond,deh}c_{p,w}t_{cond,deh} \quad (12)$$

The condensed water flow rate leaving from the dehumidifier can be calculated by

$$m^{\bullet}_{cond,deh} = m^{\bullet}_{a,o}(w_{a,deh,i} - w_{a,deh,o}) \quad (13)$$

3.4. Air conditioning system

The air conditioning system capacity (space cooling load and cooling coil load), room sensible heat factor, and condensate water over the cooling coil can be calculated from

$$Q^{\bullet}_{R} = m^{\bullet}_{a,s}(i_{a,R} - i_{a,S}) \quad (14)$$

$$Q^{\bullet}_{c,c} = m^{\bullet}_{a,s}(i_{a,cc,i} - i_{a,cc,o}) \quad (15)$$

$$RSHF = \frac{Cp_a(t_{a,R} - t_{a,s})}{(i_{a,R} - i_{a,s})} \quad (16)$$

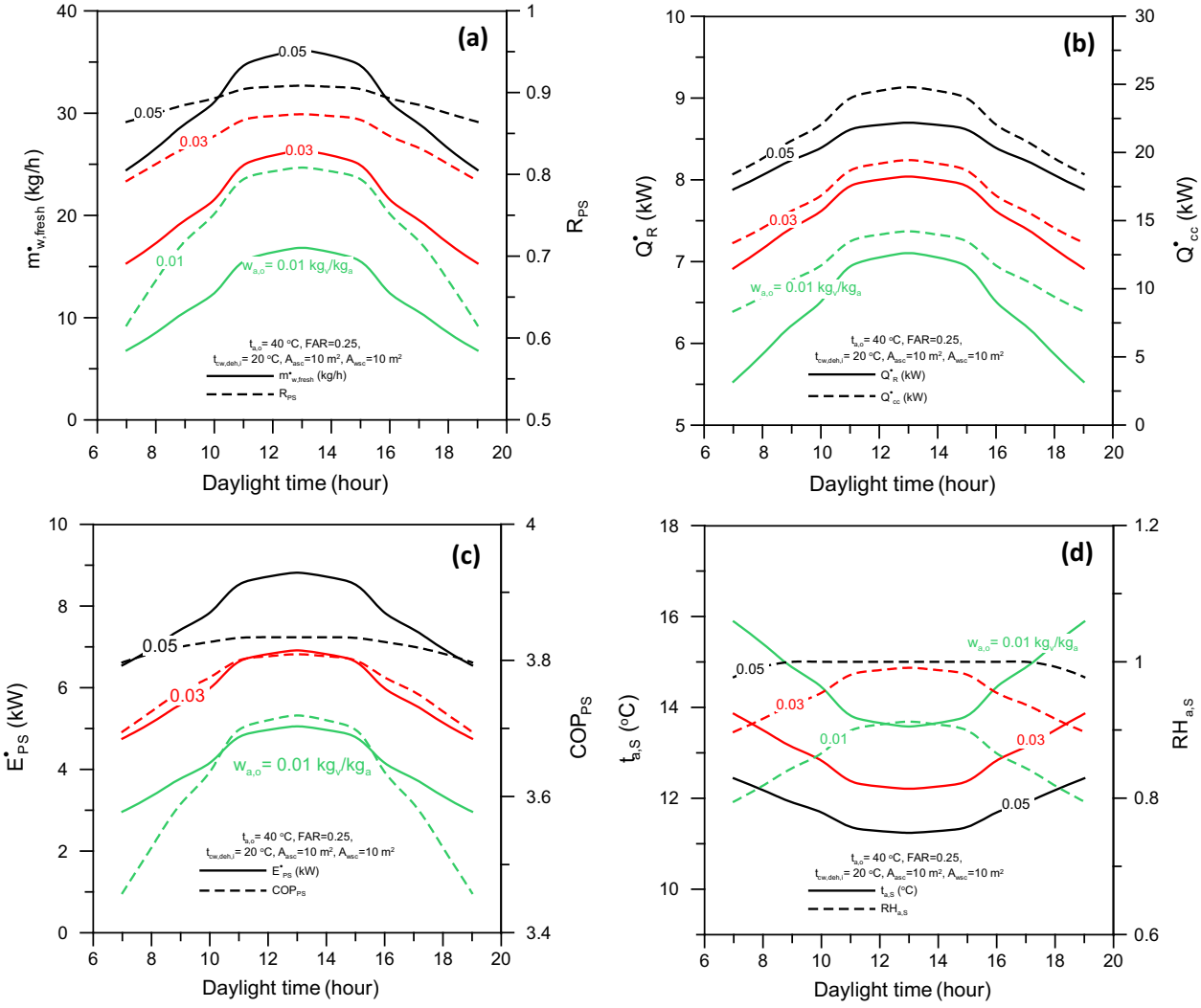

Fig. 5. Influences of the ambient humidity on the proposed system performance parameters: (a) $m^{\bullet}_{w,fresh}$ & R, (b) $Q^{\bullet}_{R}$ & $Q^{\bullet}_{cc}$, (c) $E^{\bullet}_{ps}$ & COP_{PS}, (d) $t_{a,s}$ & $RH_{a,s}$.

$$m^{\bullet}_{cond,cc} = m^{\bullet}_{a,s}(w_{a,cc,i} - w_{a,cc,o}) \quad (17)$$

where $m^{\bullet}_{a,s} = m^{\bullet}_{a,o} + m^{\bullet}_{a,Re}$.

Refrigeration unit performance coefficient in terms of ambient air temperature can be calculated by [37]:

$$COP_{Ref} = \frac{Q^{\bullet}_{c,c}}{W^{\bullet}_{c}} \quad (18)$$

$$COP_{Ref} = 11.1 - 0.4t_{a,o} + 7.2 \times 10^{-3} t^2_{a,o} - 5.18 \times 10^{-5} t^3_{a,o} \quad (19)$$

The total fresh water rate and water recovery for basic and proposed system are calculated from

$$m^{\bullet}_{w,fresh,BS} = m^{\bullet}_{cond,cc} \quad (20)$$

$$m^{\bullet}_{w,fresh,PS} = m^{\bullet}_{cond,cc} + m^{\bullet}_{cond,deh} \quad (21)$$

$$R_{BS} = \frac{m^{\bullet}_{w,fresh,BS}}{m^{\bullet}_{a,o} w_{a,o}} \quad (22)$$

$$R_{PS} = \frac{m^{\bullet}_{w,fresh,PS}}{m^{\bullet}_{makeup} + m^{\bullet}_{a,o} w_{a,o}} \quad (23)$$

Coefficient of Performance for basic and hybrid proposed systems are defined by the following equations:

$$COP_{BS} = \frac{Q^{\bullet}_{R} + m^{\bullet}_{cond,cc} h_{fg}}{E^{\bullet}_{Bs}} \quad (24)$$

$$COP_{PS} = \frac{Q^{\bullet}_{R} + m^{\bullet}_{w,fresh} h_{fg}}{E^{\bullet}_{ps}} \quad (25)$$

The total power consumption for basic and proposed systems can be given as follows:

$$E^{\bullet}_{Bs} = W^{\bullet}_{c} \quad (26)$$

$$E^{\bullet}_{ps} = W^{\bullet}_{c} + E^{\bullet}_{aux} \quad (27)$$

3.5. Operating and system design parameters

The system's capacity, consumption and performance parameters are: $m^{\bullet}_{w,fresh}$, $Q^{\bullet}_{R}$, $Q^{\bullet}_{cc}$, $E^{\bullet}_{ps}$, R, $t_{a,s}$, $RH_{a,s}$ and COP are determined as a function in all the operational and design parameters using Eqs. (1)–(27). The operating and design parameters are varied in the following range for the sake of the parametric study:

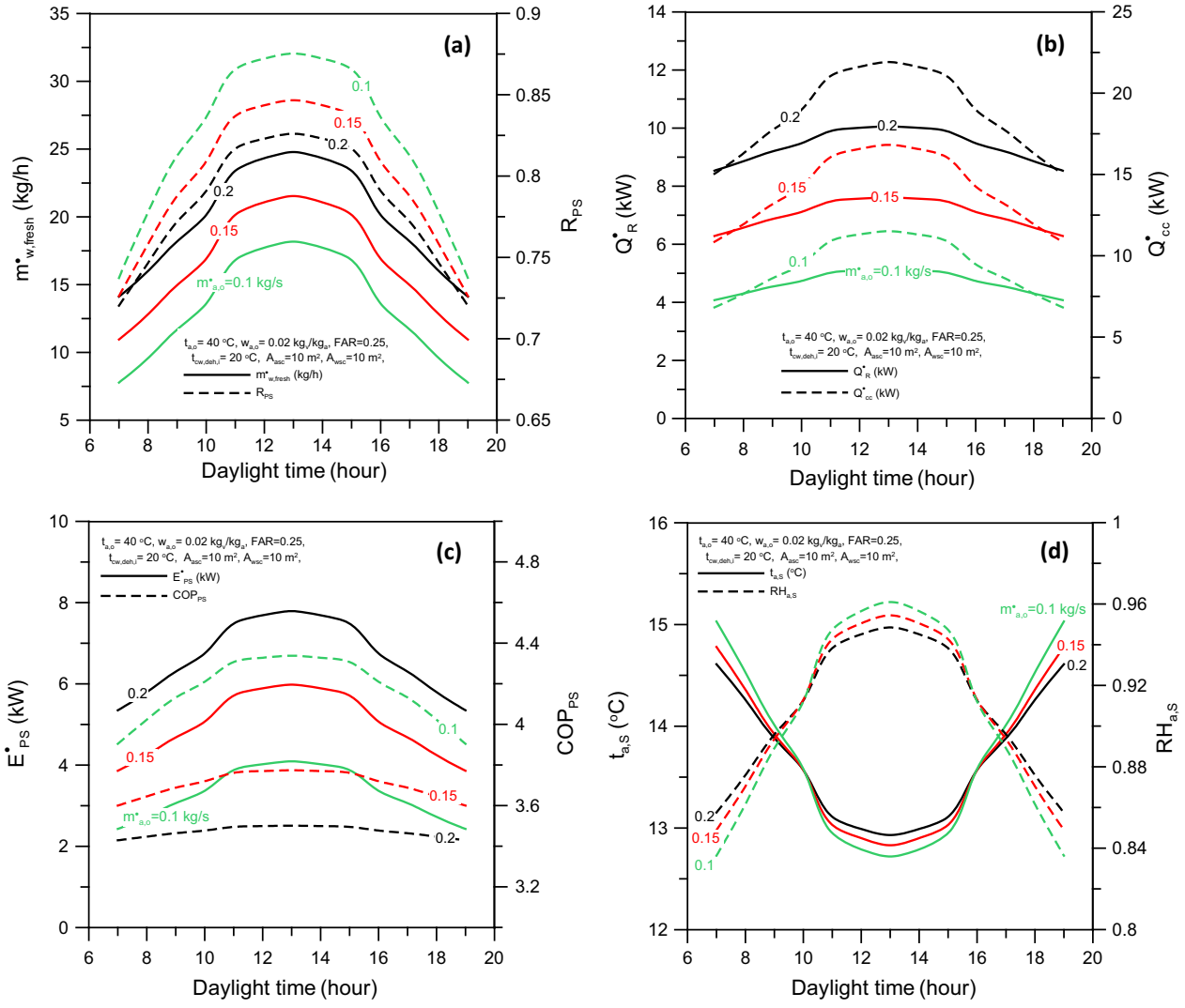

Fig. 6. Influences of the ambient air flow rate on the proposed system performance parameters: (a) $m^{\bullet}_{w,fresh}$ & R, (b) $Q^{\bullet}_{R}$ & $Q^{\bullet}_{cc}$, (c) $E^{\bullet}_{ps}$ & COP_{PS}, (d) $t_{a,s}$ & $RH_{a,s}$.

- $t_{a,o}$ = 30–50 °C (ambient air temperature)
- $w_{a,o}$ = 0.01–0.05 kg_v/kg_a (ambient air absolute humidity)
- $\dot{m}_{a,o}$ = 0.1–0.2 kg/s (air mass flow rate)
- A_{sc} = 5–15 m^2 (air and water solar collectors area)
- FAR = 0.1, 0.25, and 0.5 (fresh air ratio)
- $\dot{m}_{cw,deh}$ = 0.1–0.2 kg/s (dehumidifier cooling water mass flow rate)
- $\dot{m}_{w,h}$ = 0.1–0.2 kg/s (humidifier water mass flow rate)
- $t_{cw,deh,i}$ = 15–25 °C (dehumidifier cooling water temperature)

The air specific humilities and enthalpies that illustrated in the previous equations are calculated from air properties. The set of equations from (1)–(27) are solved numerically in the same time to conserve mass and energy for the hybrid presented system using EES software and C++ programming language.

4. Results and discussions

Hourly analysis of the system performance is investigated to present the effect of the operational and design parameters on the system performance. Finally, cost saving analysis and performance comparison study for the presented hybrid system with the basic system are conducted.

4.1. Hourly system performance

The hourly variation of proposed system performance parameters ($\dot{m}_{w,fresh}$, R, $\dot{Q}_R$, $\dot{Q}_{cc}$, $\dot{E}_{ps}$, $t_{a,s}$, $RH_{a,s}$ and COP_{PS}) are shown in Figs. 4–7 for various operational and design parameters. As shown in the figures the hourly variation of system performance follows the hourly variation of the solar radiation intensity that is shown in Fig. 3a. The figures show that $\dot{m}_{w,fresh}$, R, $\dot{Q}_R$, $\dot{Q}_{cc}$, $\dot{E}_{ps}$, $RH_{a,s}$ and COP increase with increasing the solar intensity until they reach maximum values at noon where the solar intensity is maximum then they decrease until the end of the day. The behavior of the hourly fresh water productivity and water recovery (Figs. 4a, 5a, 6a, 7a) can be attributed to the increase of the air and water temperatures exits from the solar collectors with increasing the solar intensity. Elevating air and water temperatures improve the humidification capacity (ability of the air for carrying up water vapor in the humidifier) and subsequently increases the condensate rates in the dehumidifier and the cooling coil. The hourly variation of the system cooling capacity can be attributed to the psychometric analysis which verifies the increase of the enthalpy of air leaving the humidifier (H) and consequently the increase of the enthalpy of the mixing point (M) at the same fresh air ratio. As a result, the supply air temperature drops and supply relative humidity rises (see Figs. 4d, 5d, 6d, 7d). Decreasing the supply air temperature with

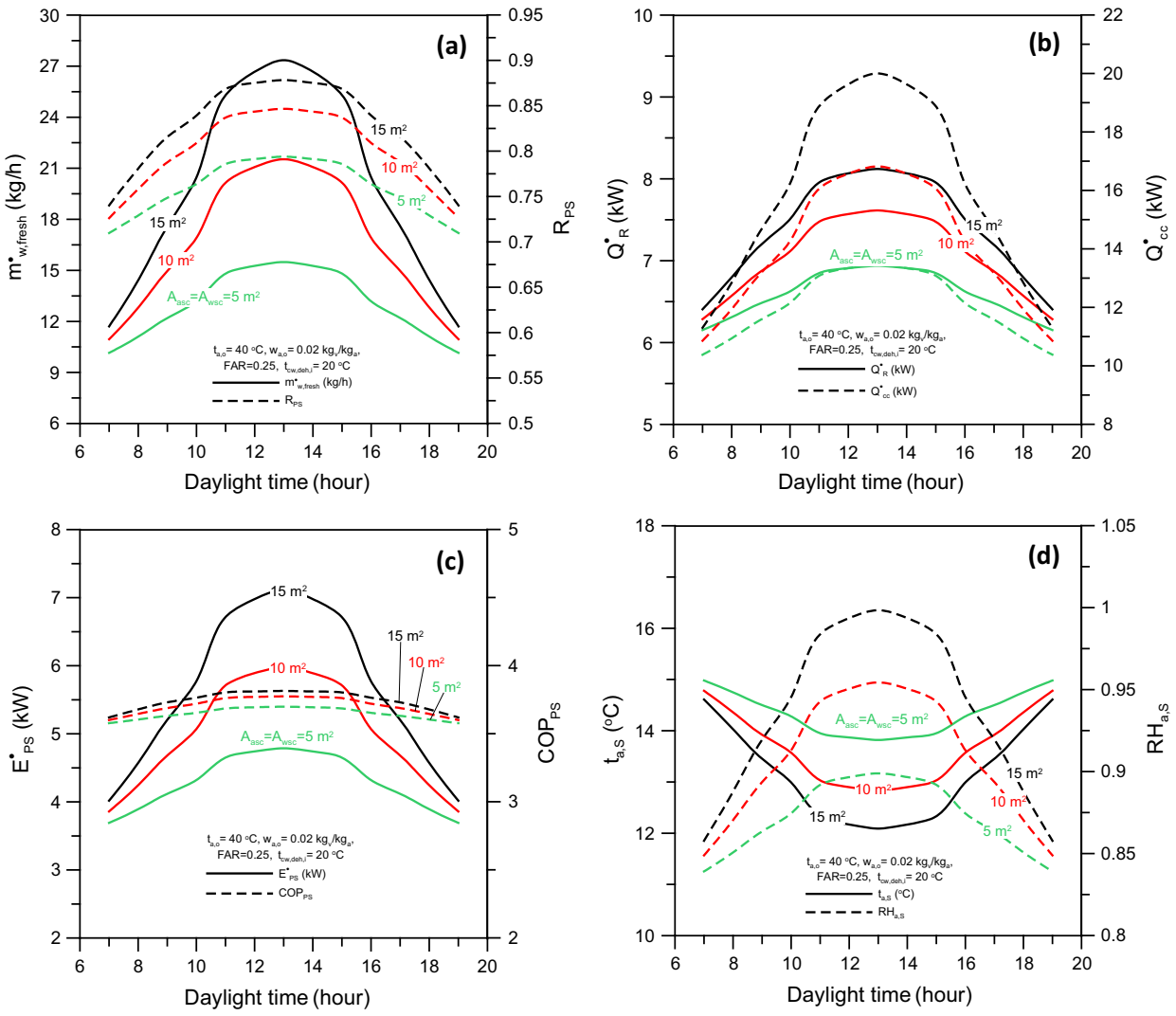

Fig. 7. Influences of solar collectors' areas on the proposed system performance parameters: (a) $\dot{m}_{w,fresh}$ & R, (b) $\dot{Q}_R$ & $\dot{Q}_{cc}$, (c) $\dot{E}_{ps}$ & COP_{PS}, (d) $t_{a,s}$ & $RH_{a,s}$.

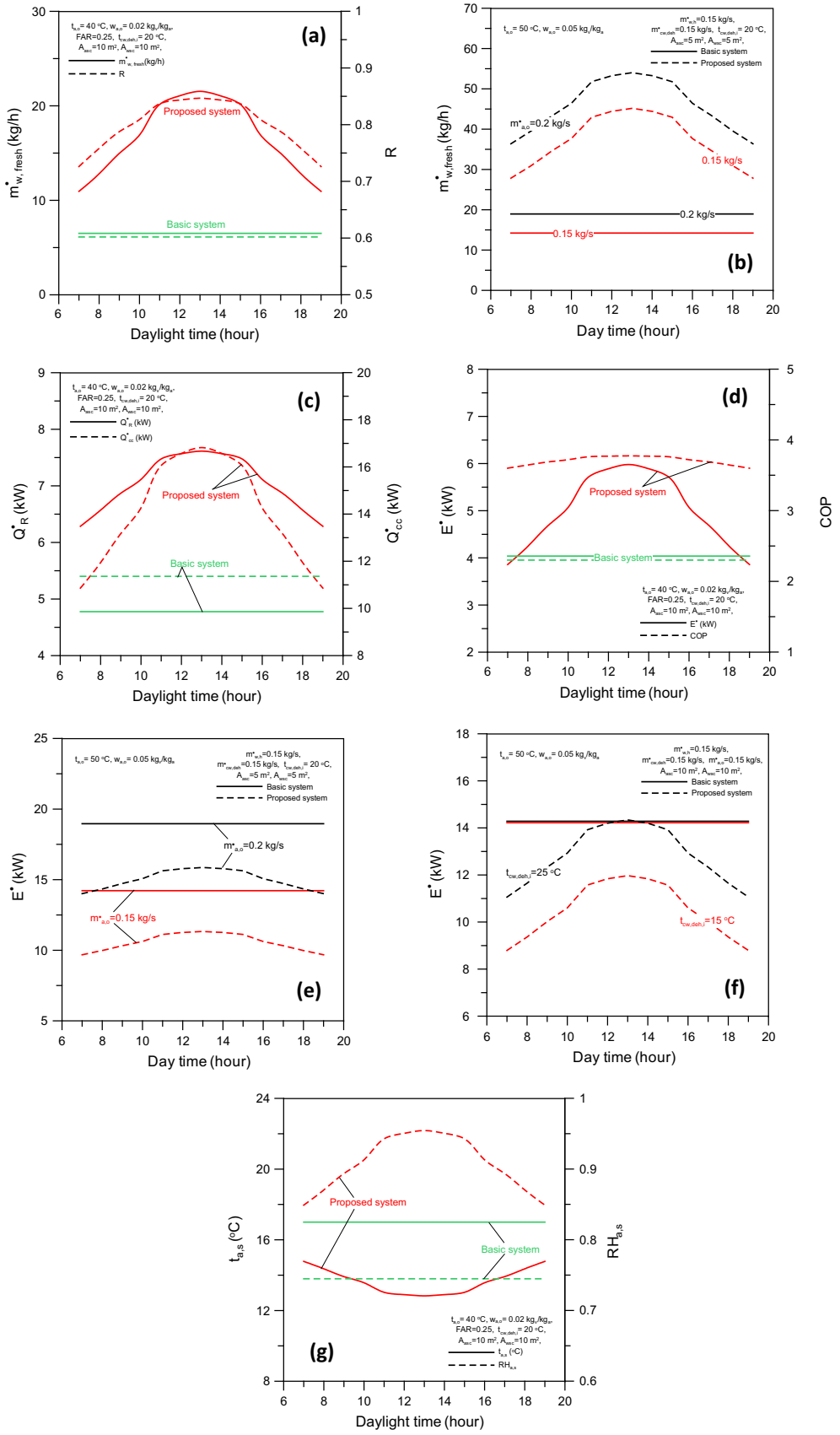

Fig. 8. Comparisons of the proposed with the basic system at different operating and design parameters.

increasing relative humidity means the drop in the enthalpy of the supply and then the increase in the building cooling load and the cooling coil capacity as shown in Figs. 4b, 5b, 6b and 7b. The increase of hourly electrical power consumption and the system COP_{PS} with the increase of the solar intensity (see Figs. 4c, 5c, 6c, 7c) can be attributed to: (i) increasing of the cooling coil capacity leads to higher electric power consumption at constant COP_{Ref} as described in Eq. (18), (ii) increasing of the system cooling capacity and the fresh water rate overcomes the increase of the system electrical power which leads to higher COP_{PS} as given by Eq. (25).

4.1.1. Effects of ambient air dry bulb temperature

The effects of ambient air dry bulb temperature on the proposed system performance parameters are shown in Fig. 4a–d for specific operating and design parameters as an example. Fig. 4a shows that the hourly fresh water production rate and the system water recovery improve with increasing the ambient air temperature. This can be attributed to the increase of air temperature at the humidifier inlet with increasing the ambient air temperature which leads to improving humidification capacity, fresh water productivity and fresh water recovery.

Fig. 4b illustrates the hourly variation of the system cooling capacity (space cooling load, $Q^{\bullet}_{R}$ and cooling coil capacity, $Q^{\bullet}_{cc}$) for different ambient air temperatures. As displayed in the figure, the system capacity increases with increasing the ambient air temperature. This can be attributed to the increase of air enthalpy at the dehumidifier outlet (k) and consequently at the mixing point (M) that lead to decreasing the supplied air enthalpy according to the psychrometric analysis. Dropping the supplied air enthalpy causes a decrease of the supplied air temperature and an increase of relative humidity to the space (see Fig. 4d) with the increase of the ambient air temperature. As explained in Section 4.1, decreasing the supply air temperature and increasing relative humidity leads to the decrease of the enthalpy of the supply air to the conditioned space and an increase in the system capacity for removing the space load. Fig. 4b also displays the improve in the cooling coil capacity with rising in ambient air temperature. This can be attributed to the rising in the system capacity and the drop in the air enthalpy downstream the cooling coil.

Fig. 4c shows the increase of the hourly electrical power consumption and the decrease of the system COP_{PS} with increasing the ambient air temperature. The increase of the electrical power consumption can be attributed to (i) the increase of the cooling coil capacity as discussed in Fig. 4b that leads to higher electric power consumption and (ii) the decrease of the chiller COP_{Ref} with the increase of the ambient air temperature (see Eqs. (18) and (19) that leads to higher electric power consumptions (see Eq. (27)). The decrease of the system COP_{PS} can be attributed to that the increase in the system cooling capacity and the fresh water rate can't overcome the increase in electrical power (see Eq. (25)).

4.1.2. Effects of ambient air absolute humidity

The effects of the ambient air humidity on the hourly variation of proposed system performance parameters are shown in Fig. 5a–d for specific operating and design parameters as an example. Fig. 5a shows that the hourly variation of $m^{\bullet}_{w,fresh}$ and R increase with increasing the humidity. The increase of the fresh water rate can be attributed to the high amount of water vapor carried by air at the humidifier's exit that leads to the increase of the driving force of mass transfer. The increase of the system water recovery with the humidity can be attributed to the increase of the fresh water rate with decreasing the make-up water (see Eq. (23)).

Fig. 5b shows that $Q^{\bullet}_{R}$, $Q^{\bullet}_{cc}$ increase with the increase of $w_{a,o}$. This is attributed to the increase of the latent heat capacities across the dehumidifier and cooling coil due to rising the air enthalpy downstream the humidifier. Rising the air enthalpy downstream the humidifier leads to an increase in the enthalpy of the mixed air (M) and a decrease in the supply air enthalpy (S) and subsequently an increase in the system capacity ($Q^{\bullet}_{R}$ & $Q^{\bullet}_{cc}$) to remove the space cooling load. This decrease the supply air temperature and increase the relative humidity as shown in Fig. 5d.

Fig. 5c displays the increase of system electric power consumption and COP_{PS} with increasing the ambient air humidity. Increasing $E^{\bullet}_{ps}$ with the increase of the $w_{a,o}$ is due to the high cooling coil capacity as discussed in Fig. 5b which results to higher electrical power consumption. The increase of the system COP_{PS} with the increasing the air humidity is due to the increase of $Q^{\bullet}_{R}$ and the fresh water productivity with a mount that overcomes on the increase in system electrical power and this leads to higher COP_{PS}.

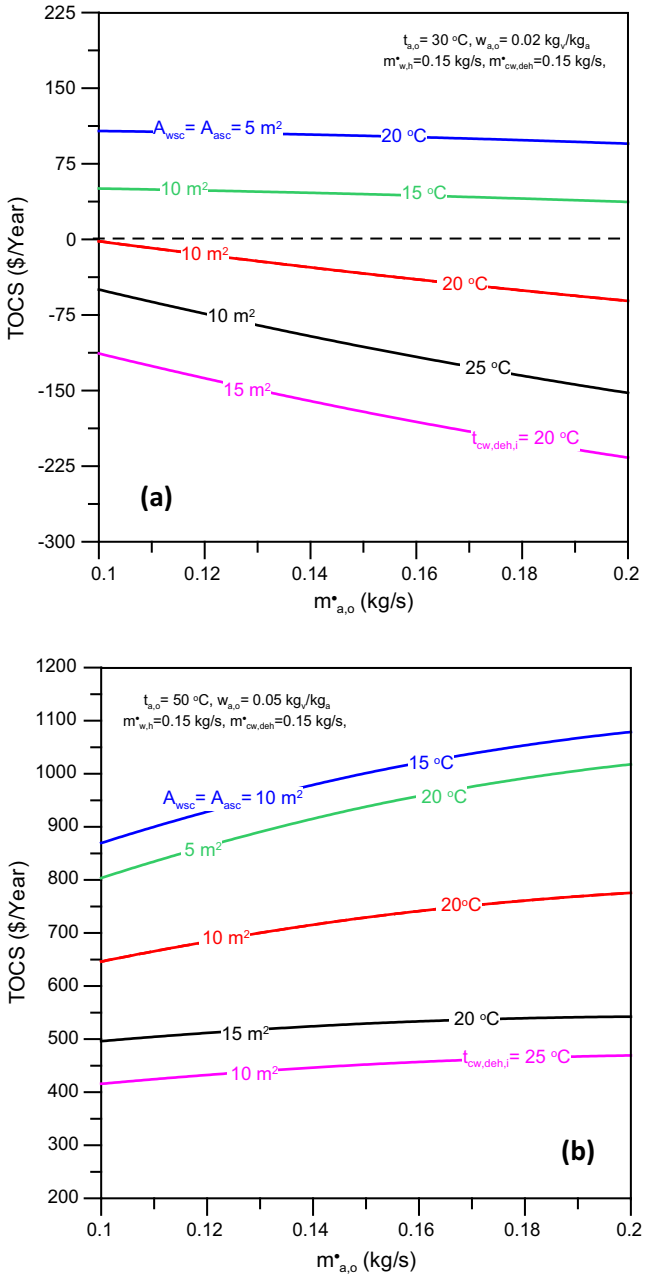

Fig. 9. TOCS: (a) influences of solar collectors' areas, (b) influences of dehumidifier inlet water temperature.

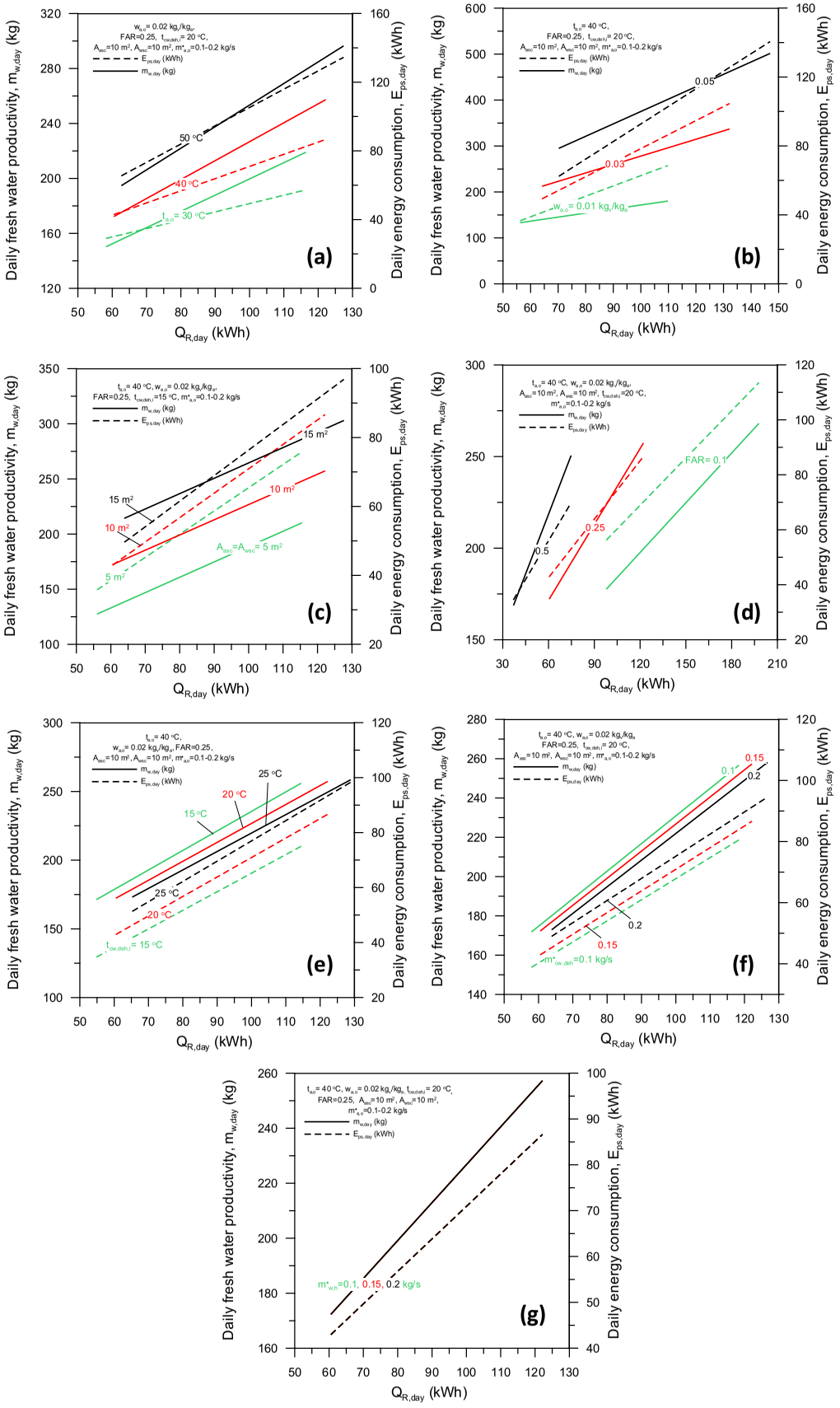

Fig. 10. Daily performance of the proposed system at different operating and design parameters.

Table 1
Constants of predicted correlations and their errors.

ψ	a	b	c	d	e	f	g	h	i	k	Error
$\frac{m^{\bullet}_{w,fresh}}{m^{\bullet}_{w,fresh,max}}$	1.282	−0.04	1.049	0.537	0.634	0.291	0.243	−0.005	−0.014	−0.014	Predicts 90% within error ±10%
$\frac{Q^{\bullet}_{R}}{Q^{\bullet}_{R,max}}$	0.117	−1.068	0.428	0.155	0.172	0.498	0.107	−0.0031	−0.118	0.265	Predicts 90% within error ±12%
$\frac{E^{\bullet}_{PS}}{E^{\bullet}_{PS,max}}$	1.087	−0.263	0.662	1.643	0.385	−0.191	0.274	0.0264	−0.221	0.569	Predicts 90% within error ±15%

4.1.3. Effects of outdoor air flow rate

The effects of the outdoor air flow rate on proposed system performance parameters are shown in Fig. 6a–d for specific operating and design parameters as an example. Fig. 6a shows the increase of $m^{\bullet}_{w,fresh}$ and the drop of R with rising $m^{\bullet}_{o,a}$. Increasing the fresh water rate with increasing $m^{\bullet}_{o,a}$ is due to the high amount of water vapor that passed through the humidifier and cooling coil which results in the increase of the amount of water vapor condensation on the dehumidifier/cooling coil surfaces. On the other side reducing the system water recovery with rising the ambient air flow rate can be attributed to that the percentage of increase of the make-up water is higher than the percentage of increase in the dehumidification capacity, $m^{\bullet}_{w,fresh}$.

Fig. 6b illustrates the increase of system cooling capacity with $m^{\bullet}_{a,o}$. This can be attributed to two opposite effects; (i) the increase of supply air flow rate with respect, (ii) the decrease in the enthalpy change through the cooling coil and conditioned space as a result of the drop in air enthalpy downstream the air solar collector. The increase in the supply air flow rate overcomes the decrease in the enthalpy difference across the cooling coil and conditioned space.

Fig. 6c illustrates the increase in the electrical power consumption and the decrease in the system COP_{PS} with decreasing the outdoor air flow rate. Increasing the system electrical power consumption can be attributed to (i) the increase of the cooling coil capacity as discussed in Fig. 6b which results to higher electrical power consumption, and (ii) the increase of the power of auxiliary system components. The decrease of the system COP_{PS} with the increase of air flow rate can be attributed to the increase of the space cooling load and the fresh water productivity with a percentage lower than the percentage of the increase in the system electrical power.

4.1.4. Effects of solar collectors' areas

The effects of the solar collectors' areas on the proposed system performance parameters are shown in Fig. 7a–d for specific operating and design parameters as an example. Fig. 7a shows the enhancement of the fresh water production rate and the system water recovery with increasing the areas of air and water solar collectors. This can be attributed to the increase of the air and water temperatures downstream the solar collectors which leads to the improve of the air humidification capacity and consequently the increase of the dehumidification capacity.

Fig. 7b shows that $Q^{\bullet}_{R}$ and $Q^{\bullet}_{cc}$ increase with increasing the solar collectors' areas. This can be attributed to the increase of the sensible heat capacities across the dehumidifier and cooling coil due to the increase of the air enthalpy downstream the air solar collector and in consequence at the humidifier's exit. Increasing of the air enthalpy at the humidifier's exit leads to high air enthalpy at mixing point (M) and low enthalpy at the supply air point (S) with keeping constant ADP and RSHF which leads to the increase of $Q^{\bullet}_{R}$ and $Q^{\bullet}_{cc}$.

Fig. 7c illustrates the increase both of the electrical power consumption and the system COP_{PS} with increasing the solar collectors' areas. Increasing the system electrical power consumption is due to the increase of the cooling coil capacity as discussed in Fig. 7b and the increase of power of auxiliary system components. The increase of the system COP_{PS} with increasing the solar collectors' areas can be attributed to the increase of the space cooling load and the system water productivity which overcomes on the increase of the system electrical power.

4.2. Comparisons and cost saving analysis

The comparison between the proposed system performance parameters and the basic system is shown in Fig. 8a–g at the operating and design parameters: FAR = 0.25, $m^{\bullet}_{a,o}$ = 0.15 kg/s, $m^{\bullet}_{w,h}$ = 0.15 kg/s, $m^{\bullet}_{cw,deh}$ = 0.15 kg/s, $A_{wsc} = A_{asc}$ = 10 m^2 and t_{cw} = 20 °C. Fig. 8a and b shows an improvement of the proposed system fresh water production rate and the system water recovery as compared with the basic system at $t_{a,o}$ = 40 °C, $w_{a,o}$ = 0.02 kg_v/kg_a, and $t_{a,o}$ = 50 °C, $w_{a,o}$ = 0.05 kg_v/kg_a, respectively. As shown in Fig. 8b, the proposed system fresh water productivity is much higher than the basic system. This is due to the existing of HDH system (humidifier/dehumidifier) with solar collectors that improve the air humidification performance.

Fig. 8c shows that the proposed system cooling capacity ($Q^{\bullet}_{R}$ and $Q^{\bullet}_{cc}$) is greater than that of the basic system along the day. This can be attributed to the increase of the air enthalpy change across the cooling coil due to elevating the air enthalpy downstream the humidifier and decreasing the supplied air temperature with rising the relative humidity (see Fig. 8g) due to existence of the HDH solar assisted system components.

Fig. 8d shows that the electrical power consumption and the COP of the proposed system are greater than those of the basic system. This can be attributed to the higher $Q^{\bullet}_{cc}$ of the proposed system as compared to the basic system (see Fig. 8c) which leads to higher electrical power consumption. The higher COP of the proposed system is attributed to the high $Q^{\bullet}_{R}$ and fresh water production rate as discussed in Fig. 7c.

Fig. 8e and f illustrates that the proposed system electric power consumption is less than that consumed in basic system at $t_{a,o}$ = 50 °C, $w_{a,o}$ = 0.05 kg_v/kg_a. The possible explanation of that is attributed to the presence of dehumidifier in the system which makes the air enthalpy at the dehumidifier's exit becomes lower than that of the outdoor air. This reduces the air enthalpy upstream the cooling coil which results in a reduction of the cooling coil capacity and the electrical power consumption.

The previous comparison study verified that the suggested system has high fresh water productivity and space cooling capacity but consumes low or high electrical power according to the operating conditions. So, for fair comparison for proposed and basic systems, the total cost savings due to fresh water productivity and electrical power consumption was selected as a judging criterion for comparison between the two systems. The TOCS is calculated as follows:

$$TOCS\ (\$/\text{Year}) = \Delta m_{w,fresh,Y}\ (\text{kg/Year}) \times Water\ unit\ rate\ (\$/\text{m}^3) + \Delta E_Y\ (\text{kW h/Year}) \times Electricity\ unit\ rate\ (\$/\text{kW h}) \quad (28)$$

where

$$\Delta m_{w,fresh,Y} = N_Y \sum_{sunrise}^{sunset} \left[m_{w,fresh,PS} - m_{w,fresh,BS} \right]$$

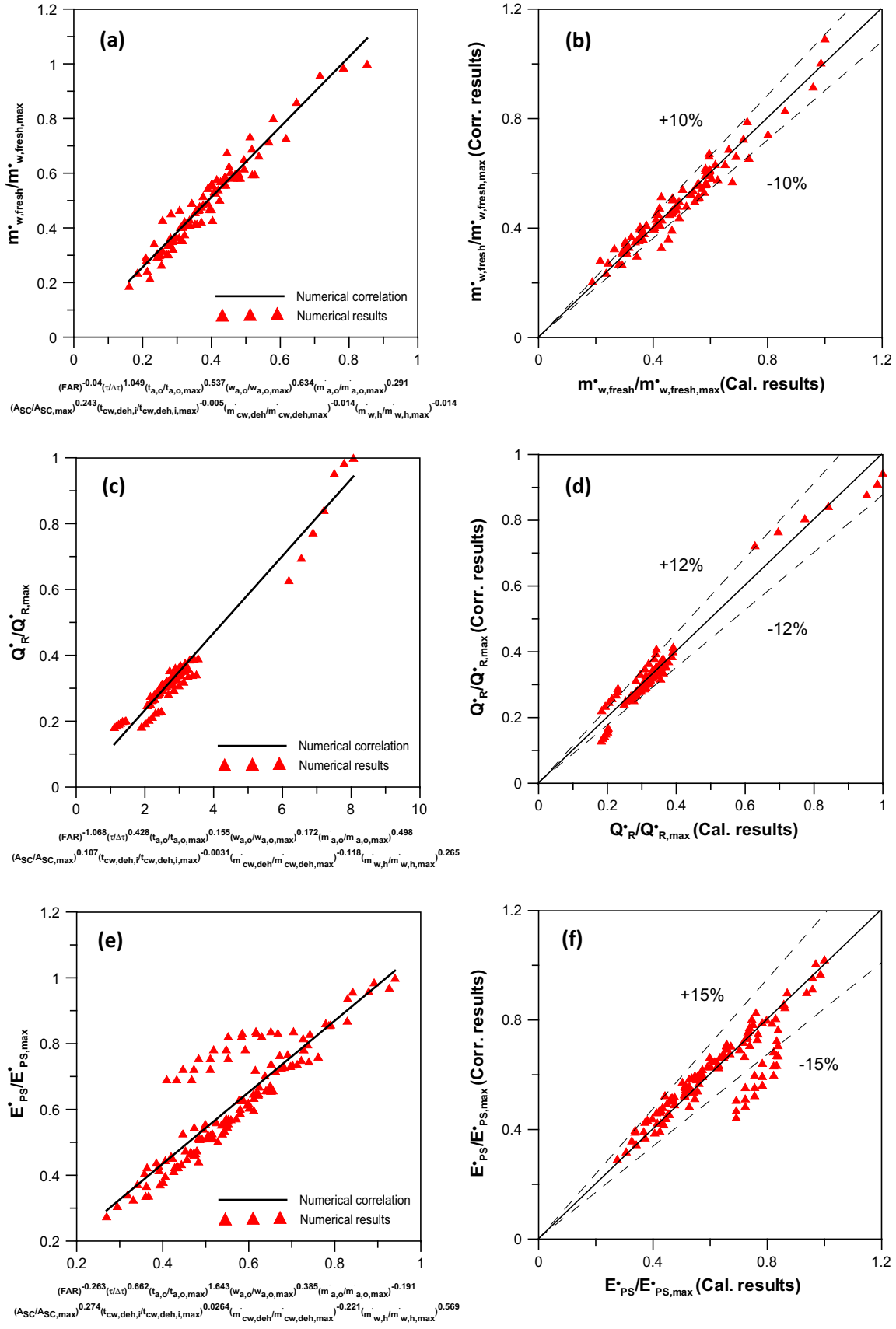

Fig. 11. Proposed system numerical correlations predictions and errors: (a & b) $\dot{m}_{w,fresh}/\dot{m}_{w,fresh,max}$, (c & d) $\dot{Q}_R/\dot{Q}_{R,max}$, (e & f) $\dot{E}_{ps}/\dot{E}_{ps,max}$.

$$\Delta E_Y = N_Y \sum_{sunrise}^{sunset} [E_{BS} - E_{PS}]$$

N_Y: Number of days a year (N_Y = 365 day).

In the current study the unit price of electrical energy and fresh water are 0.05 \$/kW h and 2.5 \$/m^3, respectively (typical values for Gulf cities [38]).

Fig. 9a and b shows TOCS versus outdoor air flow rate at $t_{a,o}$ = 30 °C, $w_{a,o}$ = 0.02 kg_v/kg_a, and $t_{a,o}$ = 50 °C, $w_{a,o}$ = 0.05 kg_v/kg_a, respectively with different operating and design parameters (A_{sc} & $T_{cw,deh,i}$). As shown in the figures, the TOCS reduces and rises with increasing $\dot{m}_{a,o}$ at $t_{a,o}$ = 30 °C, $w_{a,o}$ = 0.02 kg_v/kg_a, and $t_{a,o}$ = 50 °C, $w_{a,o}$ = 0.05 kg_v/kg_a, respectively. Reducing TOCS with rising $\dot{m}_{a,o}$ can be attributed to the higher electrical energy consumption of the proposed system and vice versa for more hot and humid conditions ($t_{a,o}$ = 50 °C, $w_{a,o}$ = 0.05 kg_v/kg_a). In addition, at low $t_{a,o}$ and $w_{a,o}$ it is observed that the proposed system operates economic deficiently relative to the basic system (see Fig. 9a). On the other side the proposed system works best economically in hot and humid climatic conditions (see Fig. 9b) and the maximum value of TOCS can be obtained throughout all the studied parameter ranges is 1079 \$/Year at A_{wsc} = A_{asc} = 10 m^2 and $T_{cw,deh,i}$ = 15 °C.

4.3. Daily system performance

The hourly system outputs and consumptions are integrated all over the day time to give the daily system output and consumptions. Fig. 10 shows the variations of the daily system outputs and consumptions for different systems capacities serving different buildings of different cooling loads. The figures are plotted for various operational and design system parameters to show their effects on the daily fresh water productivity and electrical power consumptions. Fig. 10a–g displays an improvement of the daily fresh water productivity and electrical power consumption with the increase of the integral cooling load. This can be attributed to the increase of the cooling coil capacity and the cooling load with increasing the outdoor air flow rates which results to the increase of the hourly and then daily fresh water productivity and system power electrical consumption. Fig. 10a–d illustrates enhancement of the daily fresh water productivity and electrical power consumption with increasing the ambient air temperature, the ambient relative humidity, solar collectors' areas and outdoor air flow rat, respectively. This can be attributed to the same reasons of increasing the hourly values which are discussed in Section 4.2. Fig. 10e–f shows the increase of the electrical power consumption and the decrease of the fresh water production rate with increasing both of inlet cooling water temperature and flow rates to the dehumidifier. The possible explanation can be attributed to the rising the air enthalpy downstream the dehumidifier with increasing $t_{cw,deh,I}$ and $\dot{m}_{cw,deh}$. This leads to an increase the cooling coil capacity and $\dot{E}_{ps}$. The reduction in the fresh water productivity can be attributed to the reduction in the latent heat capacity across the dehumidifier with increasing $t_{cw,deh,I}$ and $\dot{m}_{cw,deh}$. Fig. 10g shows that $\dot{m}_{w,h}$ has no effect on the electrical power consumption and fresh water productivity. The possible explanation is that the air enthalpy at the humidifier's exit remains constant with changing of $\dot{m}_{w,h}$ as the outlet water solar collector temperature decreases with increasing $\dot{m}_{w,h}$ at constant solar intensity. The maximum daily fresh water productivity, integrated cooling load and energy consumption are 501 kg, 146.7 kW h and 140 kW h, respectively at $w_{a,o}$ = 0.05 kg_v/kg_a (see Fig. 10b).

4.4. Numerical correlations prediction

To simplify and present the hourly values of $\dot{m}_{w,fresh,PS}$, $\dot{Q}_R$ and $\dot{E}_{PS}$ for proposed system, the numerical results are regressed to predict general correlations in terms of τ (time), $t_{a,o}$, $w_{a,o}$, $\dot{m}_{a,o}$, $\dot{m}_{cw,deh}$, $\dot{m}_{w,h}$, $t_{cw,deh,i}$, A_{sc}, and FAR. The developed correlations with their errors and constants are presented in Eq. (29) and Table 1 are illustrated in Fig. 11.

$$\psi = a \times FAR^b \left(\frac{\tau}{\Delta\tau}\right)^c \left(\frac{t_{a,o}}{t_{a,o,max}}\right)^d \left(\frac{w_{a,o}}{w_{a,o,max}}\right)^e \left(\frac{\dot{m}_{a,o}}{\dot{m}_{a,o,max}}\right)^f \left(\frac{A_{sc}}{A_{sc,max}}\right)^g \left(\frac{t_{cw,deh,i}}{t_{cw,deh,i,max}}\right)^h \left(\frac{\dot{m}_{cw,deh}}{\dot{m}_{cw,deh,max}}\right)^i \left(\frac{\dot{m}_{w,h}}{\dot{m}_{w,h,max}}\right)^k \quad (29)$$

Eq. (29) is valid for the following ranges 30 °C ⩽ $t_{a,o}$ ⩽ 50 °C, 0.01 kg_v/kg_a ⩽ $w_{a,o}$ ⩽ 0.05 kg_v/kg_a, 0.1 kg/s ⩽ $\dot{m}_{a,o}$ ⩽ 0.2 kg/s, 0.1 kg/s ⩽ $\dot{m}_{cw,deh}$ ⩽ 0.2 kg/s, 0.1 kg/s ⩽ $\dot{m}_{w,h}$ ⩽ 0.2 kg/s, 15 °C ⩽ $t_{cw,deh,i}$ ⩽ 25 °C, 5 m^2 ⩽ A_{sc} ⩽ 15 m^2, 0.1 ⩽ FAR ⩽ 0.5 and 7:00 ⩽ τ ⩽ 13:00 (similar and mirrored results with 13:00 ⩽ τ ⩽ 19:00). Where the values of $t_{a,o,max}$, $w_{a,o,max}$, $\dot{m}_{a,o,max}$, $\dot{m}_{cw,deh,max}$, $\dot{m}_{w,h,max}$, $T_{cw,deh,i,max}$, $A_{sc,max}$, $\Delta\tau$, $\dot{m}_{w,fresh,PS,max}$, $\dot{Q}_{R,max}$ and $\dot{E}_{PS,max}$ are 50 °C, 0.05 kg_v/kg_a, 0.2 kg/s, 0.2 kg/s, 0.2 kg/s, 25 °C, 15 m^2, 12, 36.13 kg/h, 22.24 kW and 9.092 kW, respectively.

5. Conclusions

A proposed innovated solar integrated system for A/C and HDH water desalination is proposed for climate conditions of hot and humid regions. Hourly analysis of system performance is studied using a developed mathematical model with EES and C++. System capacity parameters ($\dot{m}_{w,fresh}$, $\dot{Q}_R$ and $\dot{Q}_{cc}$) and system consumptions and performance parameters ($\dot{E}_{ps}$, R and COP) are hourly and daily estimated for various operational and design system parameters (I_T, $t_{a,o}$, $w_{a,o}$, $t_{cw,deh,i}$ and $\dot{m}_{cw,deh}$, $\dot{m}_{w,h}$, $\dot{m}_{a,o}$, FAR and A_{SC}). The results show that the main influencing parameters affecting the system's capacity, consumption and performance are $t_{a,o}$ and $w_{a,o}$. Increasing of $t_{a,o}$, $w_{a,o}$ and A_{SC} cause an increase in fresh water productivity, fresh water recovery, cooling capacity, electrical power consumption and COP of the system. TOCS parameter decreases with increasing outdoor air flow rate at $t_{a,o}$ = 30 °C, $w_{a,o}$ = 0.02 kg_v/kg_a and increases at $t_{a,o}$ = 50 °C, $w_{a,o}$ = 0.05 kg_v/kg_a. It was found that the proposed system works economically and more efficiently in hot and humid climatic conditions. The maximum TOCS can be attained from the proposed system within all the studied parameter ranges is 1079 \$/Year at $w_{a,o}$ = 0.05 kg_v/kg_a, A_{wsc} = A_{asc} = 10 m^2, $t_{a,o}$ = 50 °C, $t_{cw,deh,i}$ = 15 °C.

Moreover, the proposed system can provide maximum daily fresh water productivity and integrated cooling load with 501 kg, 146.7 kW h, respectively and consume energy with 140 kW h at $w_{a,o}$ = 0.05 kg_v/kg_a, A_{wsc} = A_{asc} = 10 m^2, $t_{a,o}$ = 40 °C, $t_{cw,deh,i}$ = 20 °C. General numerical correlations for proposed system performance parameters ($\dot{m}_{w,fresh}/\dot{m}_{w,fresh,max}$, (c) & (d) $\dot{Q}_R/\dot{Q}_{R,max}$, (e) & (f) $\dot{E}_{ps}/\dot{E}_{ps,max}$) are developed in terms of all studied design and operational parameters.

References

[1] Noreddine Ghaffour, Jochen Bundschuh, Hacene Mahmoudi, Mattheus F.A. Goosen, Renewable energy-driven desalination technologies: a comprehensive review on challenges and potential applications of integrated systems, Desalination 365 (2015) 94–114.

[2] Xing Li, Guofeng Yuan, Zhifeng Wang, Hongyong Li, Zhibin Xu, Experimental study on a humidification and dehumidification desalination system of solar air heater with evacuated tubes, Desalination 351 (2014) 1–8.

[3] Cihan Yıldırım, Ismail Solmus, A parametric study on a humidification–dehumidification (HDH) desalination unit powered by solar air and water heaters, Energy Convers. Manage. 86 (2014) 568–575.

[4] S.A. El-Agouz, G.B. Abd El-Aziz, A.M. Awad, Solar desalination system using spray evaporation, Energy 76 (2014) 276–283.

[5] H. Sharon, K.S. Reddy, A review of solar energy driven desalination technologies, Renew. Sustain. Energy Rev. 41 (2015) 1080–1118.

[6] A.E. Kabeel, Emad M.S. El-Said, A hybrid solar desalination system of air humidification dehumidification and water flashing evaporation: a comparison among different configurations, Desalination 330 (2013) 79–89.

[7] Mahmoud Shatat, Siddig Omer, Mark Gillott, Saffa Riffat, Theoretical simulation of small scale psychometric solar water desalination system in semi-arid region, Appl. Therm. Eng. 59 (2013) 232–242.
[8] Shiv Kumar, Aseem Dubey, G.N. Tiwari, A solar still augmented with an evacuated tube collector in forced mode, Desalination 347 (2014) 15–24.
[9] Xiaohua Liu, Wenbo Chen, Gu Ming, Shengqiang Shen, Guojian Cao, Thermal and economic analyses of solar desalination system with evacuated tube collectors, Sol. Energy 93 (2013) 144–150.
[10] Fahad A. Al-Sulaimana, Ifras M. Zubair, Miamoon Atif, Palanichamy Gandhidasan, Salem A. Al-Dini, Mohamed A. Anta, Humidification dehumidification desalination system using parabolic trough solar air collector, Appl. Therm. Eng. 75 (2015) 809–816.
[11] M.N.A. Hawlader, P.K. Dey, S. Diab, Solar assisted heat pump desalination system, Desalination 168 (2004) 49–54.
[12] G. Yuan, L. Zhang, H. Zhang, Experimental research of an integrative unit for air conditioning and desalination, Desalination 182 (1–3) (2005) 511–516.
[13] Shaobo Hou, Huacong Lia, Hefei Zhanga, An open air–vapor compression refrigeration system for air-conditioning and desalination on ship, Desalination 222 (1–3) (2008) 646–655.
[14] Badr A. Habeebullah, Performance analysis of a combined heat pump-dehumidifying system, JKAU: Eng. Sci. 21 (1) (2010) 97–114.
[15] J.K. Jain, D.A. Hindoliy, Experimental performance of new evaporative cooling pad materials, Sustain. Cities Soc. 1 (4) (2011) 252–256.
[16] Hanen Ben Halima, Nader Frikha, Romdhane Ben Slama, Numerical investigation of a simple solar still coupled to a compression heat pump, Desalination 337 (2014) 60–66.
[17] Ghazi Al-Enezi, Hisham Ettouney, Nagla Fawzy, Low temperature humidification dehumidification desalination process, Energy Convers. Manage. 47 (4) (2006) 470–484.
[18] A. Safwat Nafey, M.A. Mohamad, S.O. El-Helaby, M.A. Sharaf, Theoretical and experimental study of a small unit for solar desalination using flashing process, Energy Convers. Manage. 48 (2) (2007) 528–538.
[19] A.M.I. Mohamed, N.A. El-Minshawy, Theoretical investigation of solar humidification–dehumidification desalination system using parabolic trough concentrators, Energy Convers. Manage. 52 (10) (2011) 3112–3119.
[20] M.T. Ghazal, U. Atikol, F. Egelioglu, An experimental study of a solar humidifier for HDD systems, Energy Convers. Manage. 82 (2014) 250–258.
[21] Adel M. Abdel Dayem, M. Fatouh, Experimental and numerical investigation of humidification/dehumidification solar water desalination systems, Desalination 247 (2009) 594–609.
[22] Juan-Jorge Hermosillo, Camilo A. Arancibia-Bulnes, Claudio A. Estrada, Water desalination by air humidification: mathematical model and experimental study, Sol. Energy 86 (2012) 1070–1076.
[23] W.F. He, D. Han, C. Yue, W.H. Pu, A parametric study of a humidification dehumidification (HDH) desalination system using low grade heat sources, Energy Convers. Manage. 105 (2015) 929–937.
[24] C. Chiranjeevi, T. Srinivas, Experimental and simulation studies on two stage humidification-dehumidification desalination and cooling plant, Desalination 376 (2015) 9–16.
[25] Adewale Giwa, Hassan Fath, Shadi W. Hasan, Humidification–dehumidification desalination process driven by photovoltaic thermal energy recovery (PV-HDH) for small-scale sustainable water and power production, Desalination 377 (2016) 163–171.
[26] Mahmut Sami Buker, Blaise Mempouo, Saffa B. Riffat, Experimental investigation of a building integrated photovoltaic/thermal roof collector combined with a liquid desiccant enhanced indirect evaporative cooling system, Energy Convers. Manage. 101 (2015) 239–254.
[27] S.A. Nada, H.F. Elattar, A. Fouda, Experimental study for hybrid humidification–dehumidification water desalination and air conditioning system, Desalination 363 (2015) 112–125.
[28] S.A. Nada, H.F. Elattar, A. Fouda, Performance analysis of proposed hybrid air conditioning and humidification–dehumidification systems for energy saving and water production in hot and dry climatic regions, Energy Convers. Manage. 96 (2015) 208–227.
[29] H.F. Elattar, A. Fouda, S.A. Nada, Performance investigation of a novel solar hybrid air conditioning and humidification–dehumidification water desalination system, Desalination 382 (2016) 28–42.
[30] J. Yogesh, Design and Optimization of Thermal Systems, second ed., CRC Press, 2007.
[31] A.E. Kabeel, M.S. Emad El-Said, A hybrid solar desalination system of air humidification dehumidification and water flashing evaporation: a comparison among different configurations, Desalination 330 (2013) 79–89.
[32] K. Ronan McGovern, P. Gregory Thiel, G. Prakash Narayan, M. Syed Zubair, H.V. John Lienhard, Performance limits of zero and single extraction humidification-dehumidification desalination systems, Appl. Energy 102 (2013) 1081–1090.
[33] J.A. Duffie, W.A. Beckman, Solar Engineering of Thermal Process, Wiley, New York, 1991.
[34] G. Yuan, H. Zhang, Mathematical modeling of a closed circulation solar desalination unit with humidification-dehumidification, Desalination 205 (1–3) (2007) 156–162.
[35] MAZDON-HP200, Evacuated Tube Solar Energy Collector, Technical Reference & Installation Manual Domestic Hot Water, <http://www.solarthermal.com> (accessed on 31.12.11).
[36] A. Fouda, Z. Melikyan, A simplified model for analysis of heat and mass transfer in a direct evaporative cooler, Appl. Therm. Eng. 31 (2011) 932–936.
[37] YORK Catalogue, Air Cooled Screw Liquid Chillers, FORM 201.19-EG3 (803).
[38] A.A. Ahmed Attia, New proposed system for freeze water desalination using auto reversed R-22 vapor compression heat pump, Desalination 254 (1–3) (2010) 179–184.